



# **iJRASET**

International Journal For Research in  
Applied Science and Engineering Technology



---

# **INTERNATIONAL JOURNAL FOR RESEARCH**

IN APPLIED SCIENCE & ENGINEERING TECHNOLOGY

---

**Volume: 7      Issue: IV      Month of publication: April 2019**

**DOI: <https://doi.org/10.22214/ijraset.2019.4014>**

**[www.ijraset.com](http://www.ijraset.com)**

**Call:  08813907089**

**E-mail ID: [ijraset@gmail.com](mailto:ijraset@gmail.com)**

# Electrochemical Performance of Mn Doped $\text{Co}_3\text{O}_4$ Thin Film Electrodes by Electrodeposition Method

Kalyani M<sup>1</sup>, Emerson R.N.<sup>2</sup>

<sup>1,2</sup>Department of Physics, Government Arts College, Coimbatore-641018, Tamilnadu, India.

**Abstract:** *The present work is intended to prepare manganese doped cobalt oxide electrodes on copper and porous copper substrate by electrodeposited technique. Structural, morphological and electrochemical characterizations of the prepared samples were examined by using XRD, SEM, EDAX, FTIR and electrochemical measurements. Structural studies confirm  $\text{MnCo}_3\text{O}_4$  Film has face centred cubic (FCC) with polycrystalline nature. Morphological observation of the prepared films confirms the formation of nano flake like structures on copper substrates and nano rod like structures on copper porous substrates. The electrochemical performance of  $\text{MnCo}_3\text{O}_4$  electrode was tested by cyclic voltammetry, impedance and Galvanostatic charge-discharge measurements. Cyclic voltammetry observation shows films deposited on copper substrates has mixed capacitive behaviour with maximum specific capacitance of 1020 F/g and films deposited on porous copper substrates has specific capacitance of 1467 F/g at the scan rate of 10 mV/s in 1M KOH electrolyte.*

**Keywords:** *Thin films, Electrodeposition, Manganese cobalt oxide, Electrodes, Super capacitor.*

## I. INTRODUCTION

The rapid growing market in portable electronic devices and electric vehicles coupled with ever worsening global warming issues have greatly stimulated researches worldwide on exploring high-performance electrode materials for energy-storage devices [1]- [3]. Such as rechargeable batteries, fuel cells and supercapacitors as energy storage systems for electric vehicles, hybrid electric vehicles, plug-in hybrid electric vehicles and smart grids [4]- [10]. For example, lead acid batteries and lithium ion batteries as typical rechargeable batteries has been widely used as electrochemical energy storage devices and systems [11], [12]. However, most of batteries suffer from low power delivery, and cannot satisfy the faster and higher power energy requirements. In this situation, supercapacitors (SCs) were exploited to reserve and deliver energy with high rate capability, which is well adapted to provide the electricity demand for electric vehicles, diesel-engine starting, wind turbines, computers, lasers, and cranes [13], [14]. SCs, also known as ultracapacitors or electrochemical capacitors, can be fully charge-discharge only in a few seconds, leading to very higher charge/discharge power density ( $10\text{kWkg}^{-1}$ ) [15]. Obviously, the SCs are capable of perfectly fill the power energy gap between conventional dielectric capacitors with great power output and batteries owning high energy density [16], [17]. In SCs have the greatest potential in the field of energy storage devices [18]. According to the species of the electrode material and the mechanism of energy storage, generally, the supercapacitor is classified to electrical double layer capacitor (EDLC) (carbon-based materials) and pseudo-capacitor (metallic compound materials and conductive polymer materials) [19], [20]. At present, carbon-based EDLCs have been developed and employed in commerce. However, a great deal of previous work has shown that the major drawback of EDLCs is their low energy density [21]. Compared to EDLCs, pseudo-capacitors have higher energy density ascribed to the reversible redox reactions. Electrodes are the key part in supercapacitors and much work has been performed on the fabrication of electrodes [22]. Recently, a great deal of research effort has been placed on improving the performances of electrode materials such as carbon materials, transition metal oxides and conducting polymers [23]. Currently, activated carbons are the primary electrode materials for commercial supercapacitors. However, the lower specific capacitance limits their practical applications [24], [25]. Comparatively, transition metal oxides/hydroxides have been widely investigated and applied as the high-performance supercapacitor electrode materials [26], which can provide higher specific capacitance than traditional carbon based materials because of their fast reversible redox reactions caused by the multiple oxidation states. Transition metal oxides, including  $\text{RuO}_2$  [27],[28],  $\text{MnO}_2$  [29], [30],  $\text{NiO}$  [31], [32] and  $\text{Co}_3\text{O}_4$  [33], [34], have been explored as potential electrode materials used in supercapacitors in recent years due to their high pseudocapacitance caused by a fast redox reaction. Among them,  $\text{RuO}_2$  is the most prominent material reported in many literatures [27], [28] due to its high specific capacitance, good electrical conductivity and reversible charge-discharge properties. The recent work from our group has also found that  $\text{RuO}_2$  and its composite demonstrate outstanding supercapacitances under ultrafast charge and discharge with excellent rate capability and cycling stability [35]. However, the extremely high cost of  $\text{RuO}_2$  has seriously limited its practical use in supercapacitors. Therefore, it will be of great significance to develop alternative electrode materials with a low-cost and superior electrochemical performance.

In present work, we have deposited, Manganese cobalt oxide ( $MnCo_3O_4$ ), thin films from alkaline solution of cobalt chloride and manganese chloride using electrodeposition method. These electrodeposited films are characterized by X-ray diffraction (XRD) and Field Emission scanning electron microscopy (FSEM) and Energy Dispersive X-ray Analysis (EDAX) and Fourier transform infrared spectroscopy (FT-IR), Electrochemical studies of cyclic voltammetric (CV), Galvanostatic charge discharge study (GCD), Electrochemical Impedance Analysis (EIS) studies.

## II. EXPERIMENTAL DETAILS

### A. Preparation of Porous Copper Film

Porous copper was synthesized by AAO method. Xiu-Feng Han et.al [36] Vacuum coated copper thin film or any type of coated thin film is taken to the porous formation process. In present work, copper foil is chosen and it is kept in 1M of NaOH solution for about 3 minutes and dried well at room temperature. Dried film was electrodeposited in acidic electrolyte which composed of 1:4 (by volume) ratio of HCl and ethanol ( $CH_3CH_2OH$ ). Electrodeposition at acidic electrolyte is continued for 3 minutes at 12V dc power supply and dried well. Followed by this, copper foil is again electrodeposited at 0.3 M of oxalic acid solution at 30 DC power supply by maintaining  $0^\circ C$  for about 12 hours. After this process copper foil is dipped in the solution composed of 0.4M of chromic acid (3.99 g) + 0.6M of orthophosphoric acid (3.361ml) at  $60^\circ C$  temperature and dried well. [37] we have reported the Nano porous copper substrate by anodic aluminium oxide (AAO) method.

### B. Preparation of Manganese Cobalt Oxide Thin Films

Manganese cobalt oxide ( $MnCo_3O_4$ ) films are deposited onto the copper substrate and porous copper substrate by Galvanostatic electrodeposition method. Electrodeposition was carried out from an alkaline electrolyte which consists 0.1M of Manganese chloride ( $MnCl_2$ ) and cobalt chloride ( $CoCl_2$ ) at room temperature. This Solution was complexed with ammonium hydroxide ( $NH_3OH$ ), and PH of the electrolyte solution was maintained at 10. Cobalt oxide films were deposited on the cleaned copper substrate (cathode) while a Nickel electrode was used as the (anode). Manganese cobalt oxide films were deposited with a flow of direct current density of  $7\text{ mA/cm}^2$  at the deposition time of 30-45 minutes. After the deposition, electrodeposited electrode was annealed at  $300^\circ C$  for 2 hours, and this film was proceeded for characterization. The deposited amount of material on copper substrate was identified by weight difference method using a weighing balance.

### C. Thickness Measurement

The thickness of the prepared film was identified and confirmed by mass balance method. Fig.1 shows the variation of thickness ( $\text{mg cm}^{-2}$ ) with deposition time it reveals that when the number of deposition time is increased, thickness of the film also increased. Maximum thickness of  $0.45\text{ mg cm}^{-2}$  was achieved after 40 minutes of deposition time. Film deposited above 45 minutes of deposition time, leads to the formation of thicker films with the development of tensile stress in the surface and results in peeling nature. Films deposited with higher thickness was adopted for further characterizations.

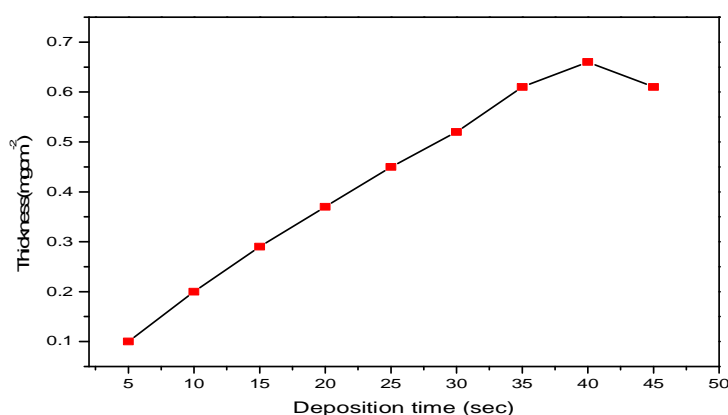


Fig.1 Thickness variation of  $MnCo_3O_4$  thin film as a function of deposition time from 10 to 40

## III. RESULT AND DISCUSSION

### A. Reaction Kinetics of the Film

The formation of Mn-doped cobalt oxide thin film electrodes are given below: Mn-doped cobalt oxide thin film.



**B. Structural Analysis**

1) *X-Ray Diffraction Technique (XRD)*: The structural properties of prepared samples were investigated and confirmed using X-Ray diffractogram in the  $2\theta$  range of  $20^\circ$ - $80^\circ$ . The X-ray diffractogram of the deposited  $MnCo_3O_4$  films on both copper and porous copper substrate annealed at  $300^\circ C$  for 2h and shown in fig. 2 (a) and (b). The diffraction peaks at  $17^\circ$ ,  $27^\circ$ ,  $43^\circ$ ,  $50^\circ$  and  $73^\circ$  are indexed as (111), (112), (400), (204), and (620) crystal plane. The obtained diffractogram indicates the presence of manganese and cobalt oxide peaks, without any other impurities in the diffraction patterns. It suggests that doped manganese ions was well incorporated into the cobalt oxide lattice site without distorting the crystal symmetry. All diffraction peaks matched well with the face-centered-cubic (fcc) (standard JCPDS no.23-1237) with a typical spinel structure. This confirms the complete transformation of  $MnCo_3O_4$ . Further, the crystallite size was estimated on the basis of full width at half maxima intensity of XRD peak by using scherrer's formula

$$D = \frac{K\lambda}{\beta \cos \theta}$$

Where D is crystalline size,  $\beta$  is full width at half maxima;  $\lambda$  is wavelength of X-ray used and  $\theta$  is diffraction angle. The average crystalline sizes are found to be as 40 nm and 48.73 nm for  $MnCo_3O_4$  films deposited on copper and porous copper substrate respectively. The crystallite size found to be quite larger than previously reported literatures [38].

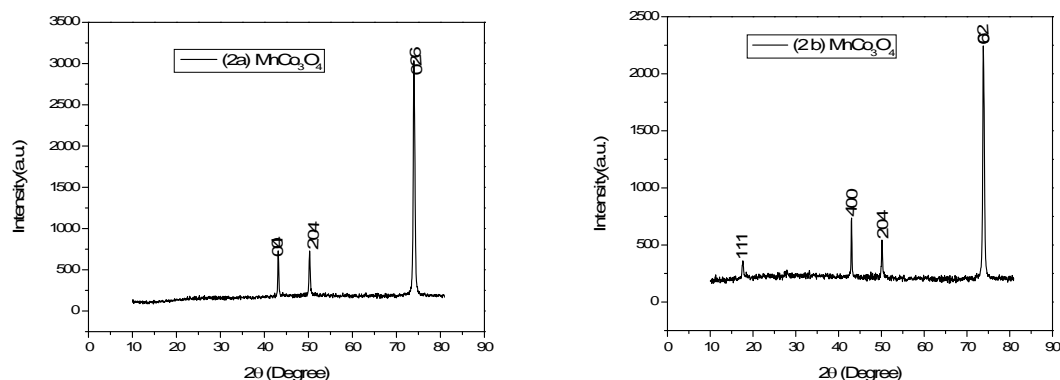


Fig. 2 The XRD Patterns of 2a.)  $MnCo_3O_4$  thin films deposited on copper substrate and 2b.)  $MnCo_3O_4$  thin films deposited on porous copper substrate.

2) *FTIR Study*: FTIR study was also evident for the structural confirmation of  $MnCo_3O_4$  films. Fig.3 (a) and (b), shows the FTIR spectra for the deposited  $MnCo_3O_4$  films on both copper and porous copper substrate studied in the range of  $4000$ - $700\text{ cm}^{-1}$ . Peaks at  $730\text{ cm}^{-1}$  can be assigned to metal-oxygen M-O vibrations of the  $MnCo_3O_4$  on copper substrate. The peaks at around  $2310$  and  $3610\text{ cm}^{-1}$  are attributed to the stretching vibration of  $CO_2$  and  $H_2O$  respectively which are originated from the exposed atmosphere. Along with the peaks assigned to carbon dioxide, some new peaks also observed in the spectrum. The bands at  $1516\text{ cm}^{-1}$  are associated with the N-H characteristic bond presented in aromatic amines [39]. The symmetric stretching vibration of C=C bond in the  $MnCo_3O_4$  rings were observed at  $1639\text{ cm}^{-1}$  [40]. In addition, the peaks located at  $810$  and  $3010\text{ cm}^{-1}$  was recognized as C-H in-plane vibration,  $832\text{ cm}^{-1}$  can be ascribed C-Cl in the plane of vibration and the N-H stretching vibrations, respectively [41].

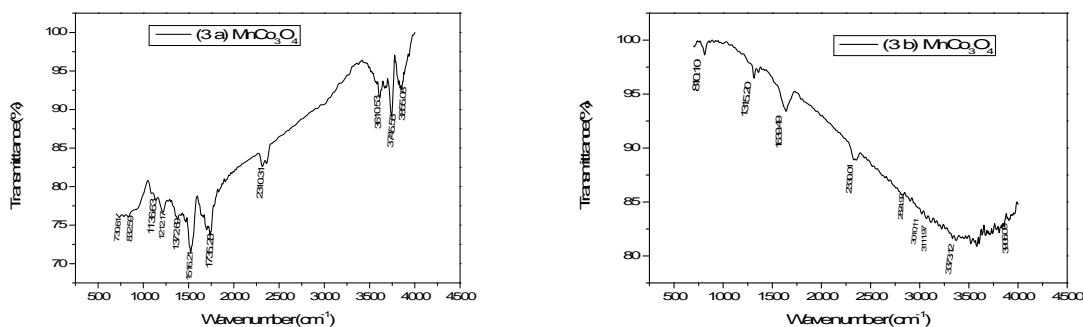




Fig. 3 FTIR spectrum of a)  $MnCo_3O_4$  thin films deposited on copper substrate b)  $MnCo_3O_4$  thin films deposited on porous copper substrate.

*C. Surface Morphological Studies (FE-SEM)*

Morphology of the  $MnCo_3O_4$  thin films deposited on both copper and porous copper substrates along with that porous formation in copper also studied and confirmed using FE-SEM micrographs and shown in Fig. 4 (a), (b), and (c). Fig. 4 (a) confirms the formation of porous on copper substrate and the average porous size is in the range of nano meter (121 nm). Micrographs of the films  $MnCo_3O_4$  films deposited on both substrates found to be as bright and uniform deposits. The films deposited on copper substrates confirms the formation of nano flake structures. The films deposited on copper porous substrates confirms the formation of nano rod like structures which may due to the enhanced deposition on porous. [42].

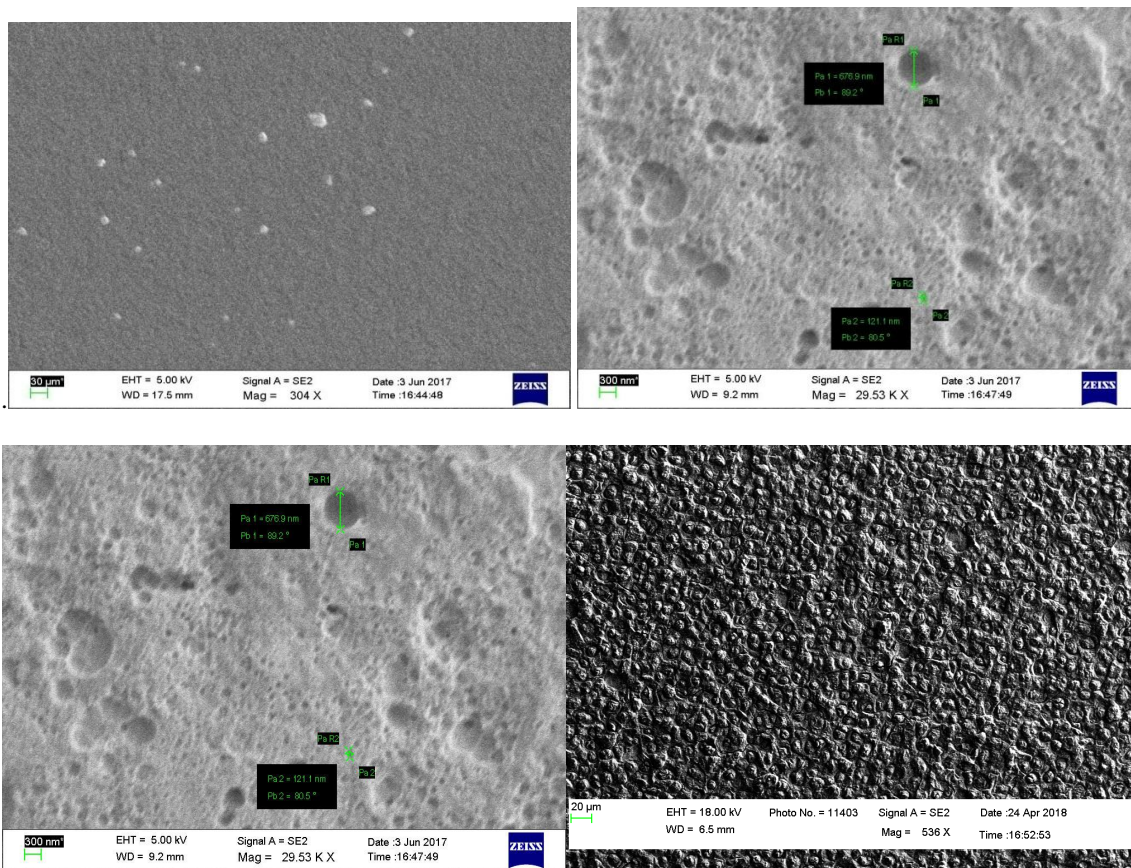


Fig. 4 (a) The scanning electron micrographs of porous copper substrate

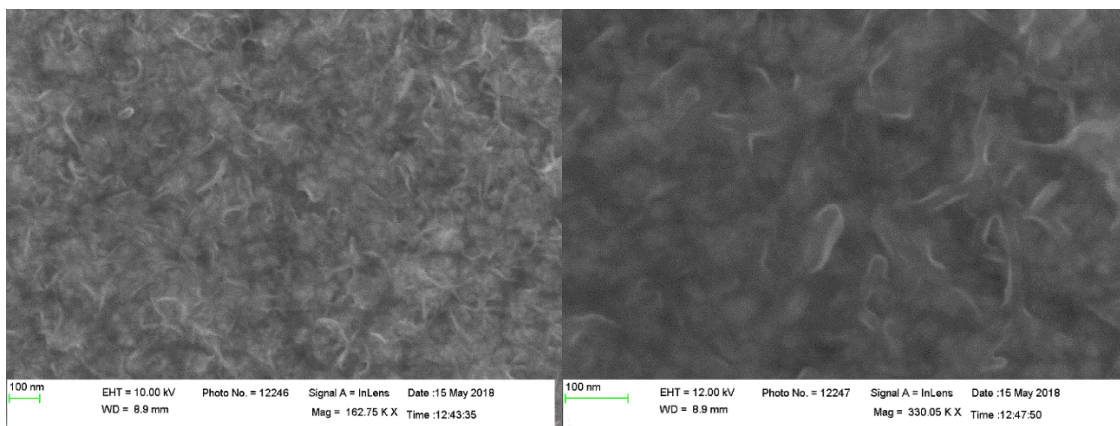


Fig. 4(b) The scanning electron micrographs of  $MnCo_3O_4$  thin film deposited on copper substrate.



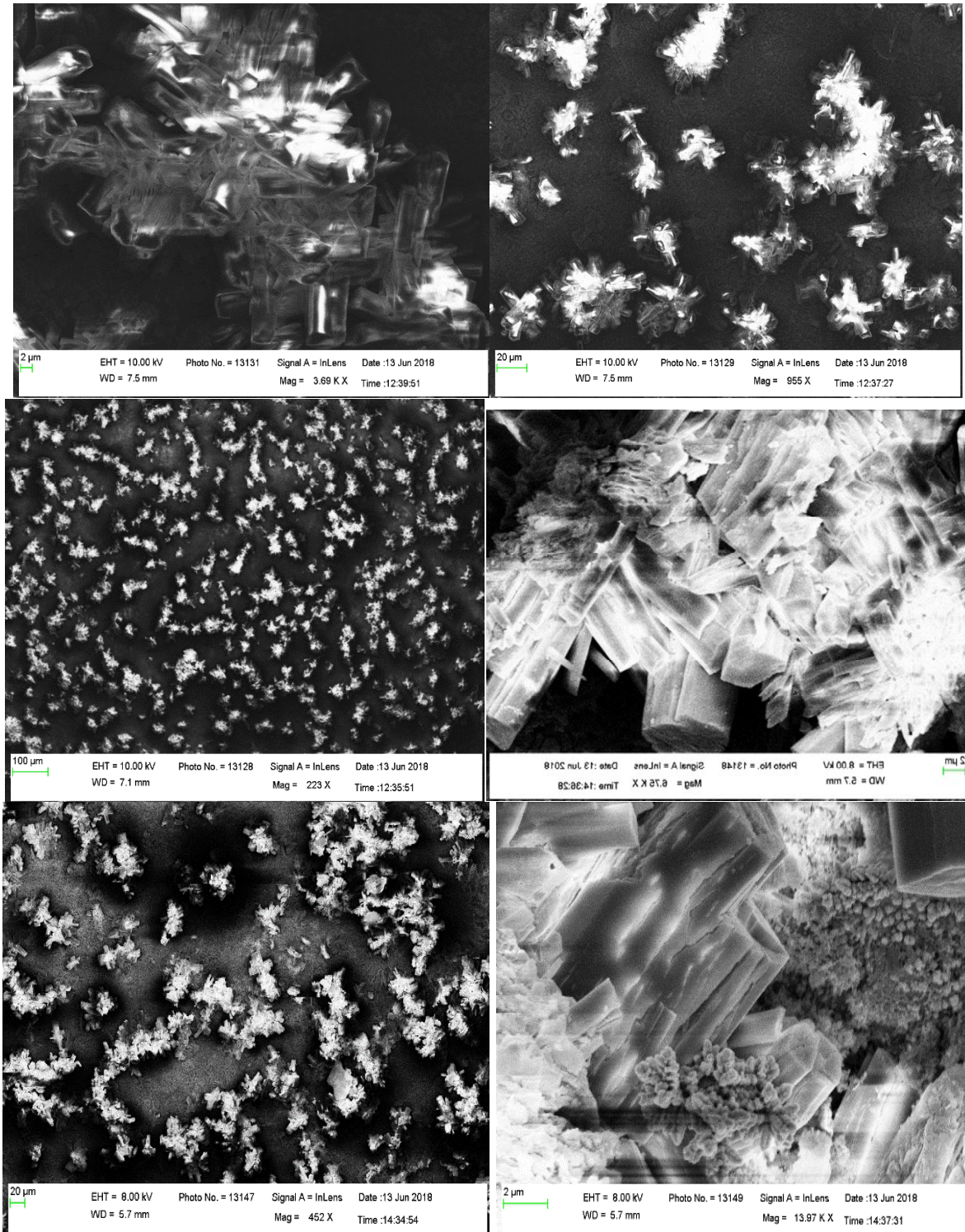


Fig. 4 (c) The scanning electron micrographs of MnCo<sub>3</sub>O<sub>4</sub> thin film deposited on porous copper substrate.

#### D. Energy Dispersive X-Ray Analysis (EDAX)

The constituents in prepared samples has been identified and confirmed by using EDAX pattern. Fig. 5(a) and (b) shows the EDAX pattern for MnCo<sub>3</sub>O<sub>4</sub> thin films deposited on copper and porous copper substrate. From this investigation the presence of Mn, Co and O elements on the films were confirmed along with substrate (Cu) peaks. Also from this analysis it is clearly confirmed that the percentage of Co, Mn atoms has been increased when the MnCo<sub>3</sub>O<sub>4</sub> films deposited on porous copper substrate which is in good agreement with the micro structural properties.

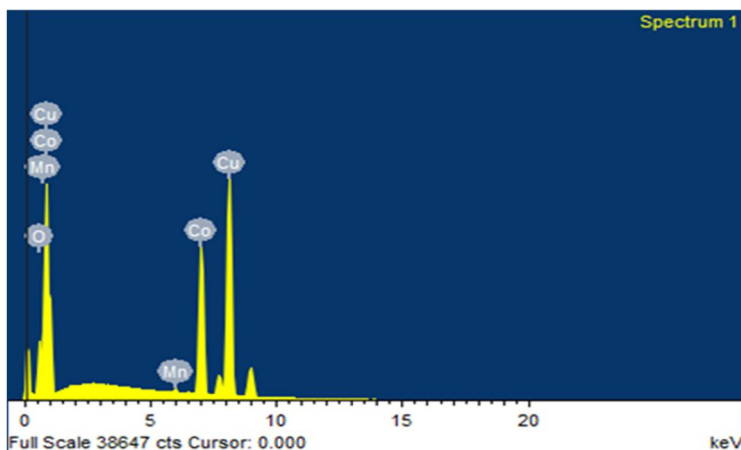


Fig. 5 (a). Energy ray dispersive analysis of  $\text{MnCo}_3\text{O}_4$  thin films deposited on copper substrate.

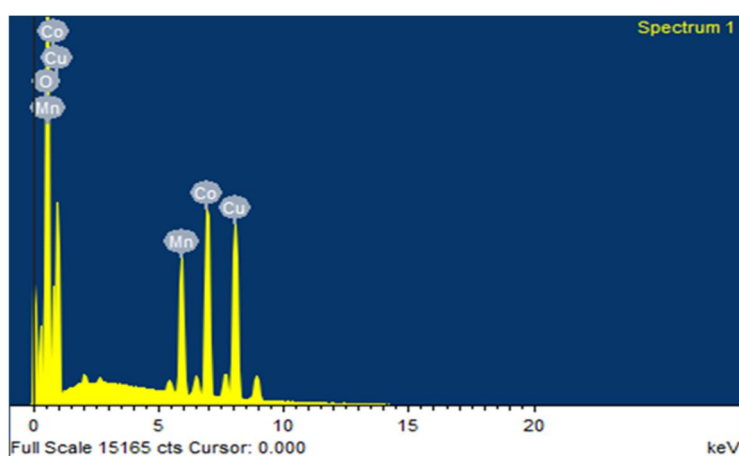


Fig. 5 (b). Energy ray dispersive analysis of  $\text{MnCo}_3\text{O}_4$  thin films deposited on porous copper substrate.

### E. Supercapacitive Study

1) *Cyclic Voltammetry (CV)*: Cyclic Voltammetry used to characterize capacitive behaviour of an electrode material. Using Cyclic Voltammogram electrochemical performance of  $\text{MnCo}_3\text{O}_4$  thin film electrodes deposited on both copper and porous copper substrates was studied. Cyclic voltammogram of  $\text{MnCo}_3\text{O}_4$  thin films in 0.1 M of KOH solution with a scan rate of 10-100 mV/s are given in fig. 6 (a) and (b). A single redox couple was observed during the scan process and the obtained cyclic voltammograms are in good agreement with earlier reports [43], [44]. The potential window used for scanning process is swept from -0.6 to +0.6 V for  $\text{MnCo}_3\text{O}_4$  films. Manganese doped cobalt oxide ( $\text{MnCo}_3\text{O}_4$ ) layers exhibits an enhancement in the current density of the anodic and cathodic peaks at the cost of the reduction in the potential window was observed. Similar type of observation was also made by Naveen and Selladurai [45]. The possible reason for this unusual behaviour could be due to promotion of ionic conductivity of  $\text{Co}_3\text{O}_4$  film upon Mn doping. It is worth to mentioning that no addition peaks were observed corresponding to manganese even at higher dopant concentration, which signifies that manganese, does not have any contribution to the electrochemical activity. As per the performance of supercapacitor electrode is concern, electrochemical redox activity plays a vital role to increase the pseudo-Faradaic surface redox reaction using different electrolytes, also electrolyte ionic size plays very important role in ionic conductivity. All CVs are nearly rectangular double layer nature having small oxidation reduction peaks indicating mixed capacitive behaviour of the prepared electrodes. The shape of CV curves deviated from the ideal rectangular shape of electric double layer reveal the obvious feature of faradic capacitance, displaying strong redox behaviour. The redox peaks shifted with an increase of scan rate, indicating the quasi-reversible feature of the redox couples, which is related to intercalate mechanism of the  $\text{OH}^-$  ions at the interface of electrode/electrolyte under higher scan rate. Likewise, the peak current densities increased with the increase of the scan rates from 10 to 100 mV/s, which suggests its good reversibility of fast charge/discharge response. Figure 7 shows the specific capacitance values it is found to be decreased when the scan is increased which is comparable with the values reported in the previous literatures. Naveen et al. [45] reported the value of capacitance as  $440 \text{ Fg}^{-1}$ . R.C. Ambare et al.,  $485 \text{ Fg}^{-1}$ . Doping cobalt ions into the manganese oxide system may be an important factor in increasing the specific capacity [46]. In present case  $\text{MnCo}_3\text{O}_4$  films on copper substrate showed

maximum specific capacitance as  $1020 \text{ Fg}^{-1}$  and  $\text{MnCo}_3\text{O}_4$  films on porous copper substrate showed maximum specific capacitance as  $1467 \text{ Fg}^{-1}$ . Hence, from the above electrochemical parameters the  $\text{MnCo}_3\text{O}_4$  electrode prepared via electrodeposition method showed excellent supercapacitive performance. The specific capacitance of the electrode, based on CV curves, can be calculated as

$$C = (\int I dv) / v mV$$

Where, C is the SC of electroactive materials ( $\text{F g}^{-1}$ ), I is the response current (A), V is the potential (V), v is the potential scan rate ( $\text{V s}^{-1}$ ), and m is the mass of the electrode materials (g).

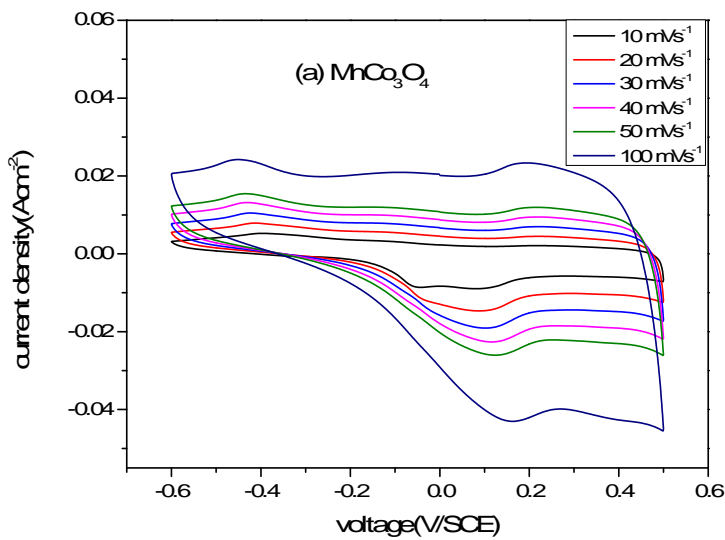


Fig. 6 (a). The curve of  $\text{MnCo}_3\text{O}_4$  thin film electrode deposited on copper substrate at different scan rate in 1M KOH electrolyte.

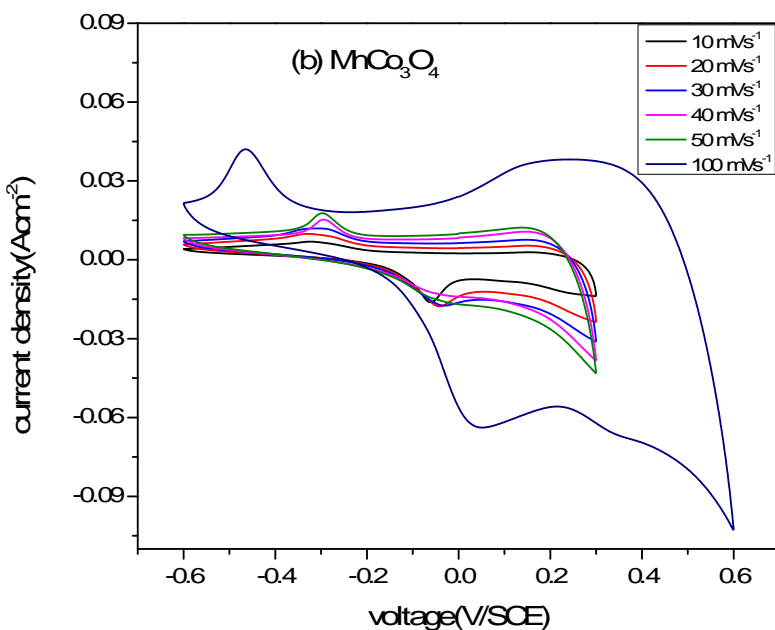


Fig. 6 (b). The curves of  $\text{MnCo}_3\text{O}_4$  thin film electrode deposited on porous copper substrate at different scan rate in 1M KOH electrolyte.



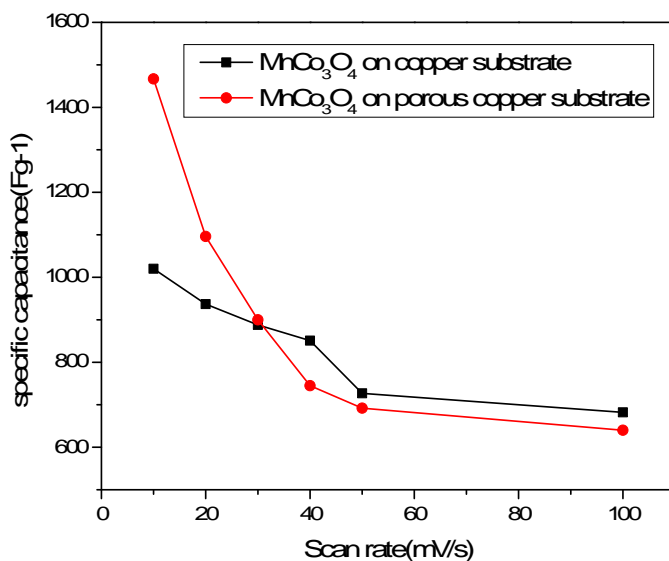


Fig. 7 The variations of specific capacitance values deposited MnCo<sub>3</sub>O<sub>4</sub> thin film electrode on both copper substrate and Porous copper substrate at different scan rate in 1M KOH electrolyte.

2) *Galvanostatic Charge Discharge Study(GCD)* : The charge-discharge curves of the MnCo<sub>3</sub>O<sub>4</sub> electrode on both copper and porous copper substrate shown in fig. 8 (a) and (b) which is taken using Chrono potentiometric technique at the potential range - 0.2 and 0.6 V at various current densities of 1, 3, 5 mA/cm<sup>2</sup> in 1M KOH electrolyte. It is observed that charge discharge time of the electrode decreases with respect to the current density. At 5mA/cm<sup>2</sup> sample shows nearly symmetric behaviour. The linear decrease in the potential drop (ohmic drop) itself indicates the pseudo capacitive behaviour of the prepared electrode. It is also reveals that an increase in current density causes a small curve shift towards nearly symmetric behaviour. From the discharge curves, specific capacitance value was calculated using the following equation:

$$C = (I \Delta t) / (m \Delta v)$$

Where, C is the Specific capacitance of the active materials (F g<sup>-1</sup>), I is the constant discharge current (A),  $\Delta t$  is the discharge time (s),  $\Delta v$  is the voltage change after a full discharge (V), and m is the mass of the active material (g), respectively. The calculated specific capacitances of MnCo<sub>3</sub>O<sub>4</sub> thin film on copper substrate electrode are 953, 750 and 625 F g<sup>-1</sup> at discharge current densities of 1,3,and 5 m A/cm<sup>2</sup> and MnCo<sub>3</sub>O<sub>4</sub> thin film on porous copper substrate electrode are 1125, 825 and 710 F g<sup>-1</sup> at discharge current densities of 1,3,and 5 m A/cm<sup>2</sup>, respectively. Fig. 9 shown in the capacitance decreases with an increase in the discharge current densities, which may be described to the increment voltage drop and relatively in sufficient active material involved in redox reaction under higher current densities.

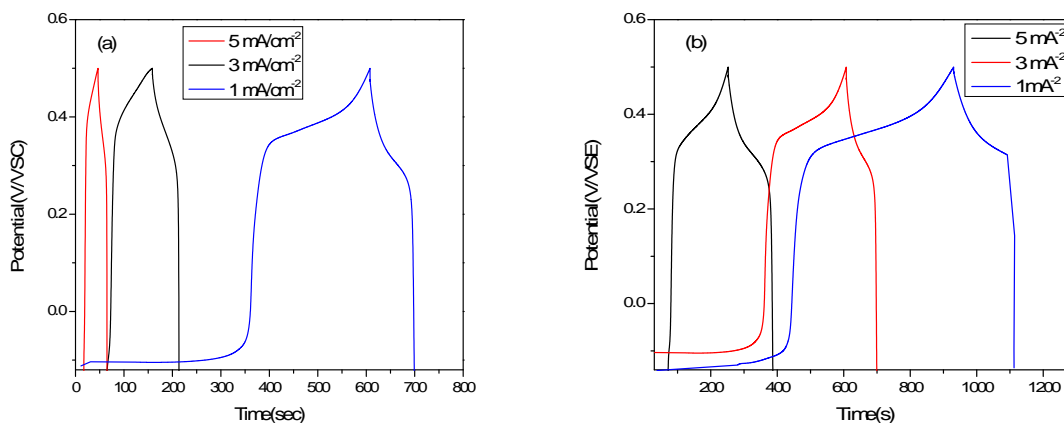


Fig. 8 a) Galvanostatic charge-discharge curves of  $\text{MnCo}_3\text{O}_4$  thin film electrode deposited on copper substrate and 8b) Galvanostatic charge-discharge curves of  $\text{MnCo}_3\text{O}_4$  thin film electrode deposited on porous copper substrate at various current densities in 1M KOH electrolyte.

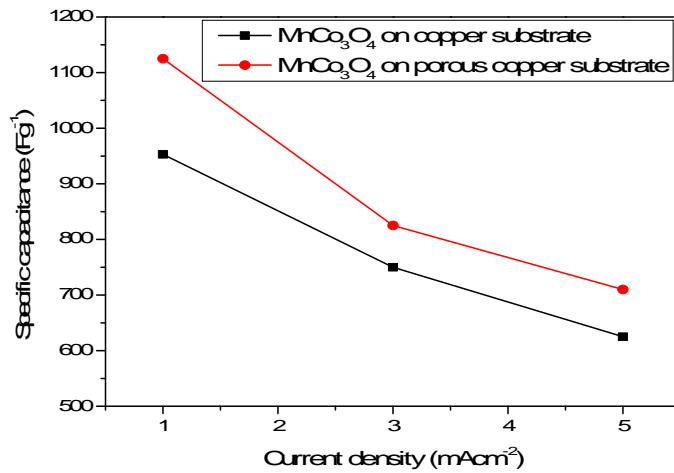


Fig. 9. The variations of specific capacitance values deposited  $\text{MnCo}_3\text{O}_4$  thin film electrode on both copper substrate and Porous copper substrate at different scan rate in 1M KOH electrolyte.

3) *Electrochemical Impedance Spectroscopy (EIS)*: Electrochemical impedance spectroscopy data were studied to quantify the electronic and ionic conductivities and diffusive behaviour of the  $\text{MnCo}_3\text{O}_4$  thin films. Nyquist plots of annealed samples  $\text{MnCo}_3\text{O}_4$  electrodes were studied in 1M KOH electrolyte.  $\text{MnCo}_3\text{O}_4$  electrode were subjected to AC impedance measurement in the range of 1 Hz – 1000 Hz at their respective open circuit potentials. Fig. 10 (a) and (b) shows the complex plane impedance plots or Nyquist plots drawn imaginary part  $Z''$  against the real part  $Z'$  for charge-discharge process. Near absence of semicircle in the high frequency region depicts the low internal resistance of the electrode materials and diffusion controlled rate kinetics of the redox process. The EIS figures show the small semicircle (first segment), Warburg diffusion line (second segment) and capacitive line (third segment). The beginning of the semicircle line (left-intercept of  $Z''$  at the  $Z'$  axis) represents the resistance ( $R_s$ ) of the electrolyte incontact with the current collector and electrode. The termination of the semicircle line (right-intercept of  $Z''$  at the  $Z'$  axis) represents the internal resistance ( $R_p$ ) of the electrode. The diameter of the semicircle ( $R_p - R_s$ ) is equal to the ESR value. The second segment (straight line with a slope of approximately  $45^\circ$ ) in the middle frequency region represents the combination of resistive and capacitive behaviours of the ions penetrating into the electrode pores. The length, slope and position of this segment appear to be different with each electrolyte. The third segment (straight lines sharply increasing at the low-frequency region) represents the dominance of capacitive behaviour from the formation of ionic and electronic charges of the electric double layer system at the micro pore surfaces at this frequency, the ions can more easily diffuse into the micro pores.

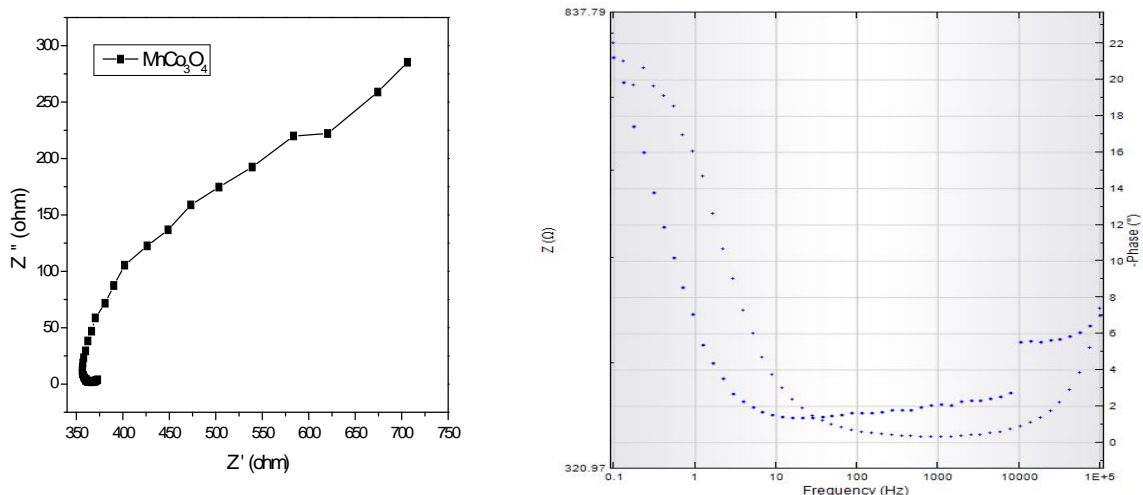


Fig. 10 a) and b). Impedance analysis of  $\text{MnCo}_3\text{O}_4$  thin film electrode at 1M KOH electrolyte.

#### IV. CONCLUSION

The Mn doped  $\text{Co}_3\text{O}_4$  thin film was prepared by Electrodeposition (galvanostatic method) technique on both copper and porous copper substrate. The obtained diffractogram indicates the presence of manganese and cobalt oxide peaks, also there is no impurity peaks are observed. It suggests that doped manganese ions have been well incorporated into the cobalt oxide lattice site without distorting the crystal symmetry. FESEM micrographs confirm the formation of porous and uniform film deposition on both substrates with nano structures. EDAX spectra of the prepared films clearly confirmed that the presence of Co, Mn atoms with increase in their elemental percentage when the deposited films is annealed. FT-IR spectra confirms the presence of all functional groups corresponding to the Manganese cobalt oxide. The  $\text{MnCo}_3\text{O}_4$  thin film electrode deposited on copper substrates showed super capacitive behaviour with maximum value of specific capacitance  $1020 \text{ Fg}^{-1}$  and films deposited on porous copper substrates showed excellent super capacitive behaviour with maximum value of specific capacitance  $1467 \text{ Fg}^{-1}$  at the scan rate  $10 \text{ mV/s}$  in  $1 \text{ M KOH}$  electrolyte. The good stability in charge discharge property on  $\text{MnCo}_3\text{O}_4$  on porous copper substrate electrode is confirmed, which also shows high specific capacitance values compared to  $\text{MnCo}_3\text{O}_4$  on copper substrate electrode. From this research work it is concluded that, electrodeposition found to be an ideal and economical technique for preparing manganese cobalt oxide electrode.  $\text{MnCo}_3\text{O}_4$  films deposited on porous copper substrate exhibit better electro capacitive behaviour which can be adaptable for supercapacitor application.

#### REFERENCES

- [1] J. R. Miller, P. Simon, Electrochemical Capacitors for Energy Management Science, 321 (2008) 651-652.
- [2] P. Simon, Y. Gogotsi, Materials for electrochemical capacitors Nature of Material. 7 (2008) 845-854.
- [3] I. Hadjipaschalis, A. Poullikkas, V. Efthimiou, Overview of current and future energy storage technologies for electric power applications, Renewable and Sustainable Energy Reviews. 13 (2009) 1513-1522.
- [4] S. Chu, A. Majumdar, Opportunities and challenges for a sustainable energy future, Nature, 488 (2012) 294-303.
- [5] J. Lv, T. Liang, M. Yang, S. Ken, M. Hideo, Low-cost treated anode for lithium-ion battery:  $\text{MnO}@\text{C}$ , Journal of Energy Chem. 26(2017) 330-335.
- [6] B. D. Boruah, A. Misra, A flexible ternary oxide based solid-state supercapacitor with excellent rate capability, Journal of Material Chemistry. A4 (2016) 17552-17559.
- [7] Y. Tu, D. Deng, X. Bao, Carbon-Based Metal-Free Catalysts: Design and Applications Journal of Energy Chemistry, 25(2016)957-966.
- [8] T. Brezesinski, J. Wang, S. H. Tolbert, B. Dunn, Ordered mesoporous  $\alpha\text{-MoO}_3$  with iso-oriented nano crystalline walls for thin-film pseudocapacitors. Nature Materials, 9(2010) 146-151.
- [9] C. Liu, F. Li, L. P. Ma, H. M. Cheng, Advanced materials for energy storage, Journal of Advance Materials, 22 (2010) E28-E62.
- [10] Q. Zhang, B. Zhao, J. Wang, C. Qu, H. Sun, K. Zhang, M. Liu, Green synthesis of cobalt (II, III) oxide nanoparticles using Moringa Oleifera natural extract as high electrochemical electrode for supercapacitors, Nano Energy 28(2016)475-485.
- [11] M. Armand, J. M. Tarascon, Building Better Batteries, Journal of Nature, 451 (2008) 652-657.
- [12] M. S. Whittingham, Lithium Batteries and Cathode, Journal of Materials Chemistry Review, 104 (2004) 4271-4302.
- [13] B. E. Conway, Transition from "Supercapacitor" to "Battery" Behavior in Electrochemical Energy Storage, Journal of Electrochemical Science, 138 (1991) 1539-1548.
- [14] E. Frackowiak, Carbon materials for supercapacitor application, Journal of Physical Chemistry, 9(2007)1774-1785.
- [15] H. Jiang, P. S. Lee, C. Li, 3D carbon based nanostructures for advanced supercapacitors, Energy Environmental Science 6(2013)41-53.
- [16] C. Largeot, C. Portet, J. Chmiola, P. L. Taberna, Y. Gogotsi, P. Simon, Relation between the Ion Size and Pore Size for an Electric Double-Layer Capacitor, Journal of Am. Chem. Soc. 130(2008)2730-2731.
- [17] J. Yan, Q. Wang, T. Wei, Z. Fan, Three-dimensional  $\text{NiCo}_2\text{O}_4@ \text{NiWO}_4$  core-shell nanowire arrays for high performance supercapacitor, Advance Energy Mater. 4 (2014) 157-164.
- [18] Z. Yu, L. Tetard, L. Zhai, J. Y. Thomas, Supercapacitor electrode materials: nanostructures from 0 to 3 dimensions, Energy Environ. Sci. 8 (2015) 702-730.
- [19] J. H. Zhong, A. L. Wang, G. R. Li, J. W. Wang, Y. N. Ou, Y. X. Tong,  $\text{Co}_3\text{O}_4/\text{Ni}(\text{OH})_2$  composite mesoporous nanosheet networks as a promising electrode for supercapacitor applications, Journal of Materials Chemistry, 22(2012)5656-5665.
- [20] Y. W. Wang, L. Yu, X. W. Lou, Formation of Triple-Shelled Molybdenum-Polydopamine Hollow Spheres and Their Conversion into  $\text{MoO}_2/\text{Carbon}$  Composite Hollow Spheres for Lithium-Ion Batteries, Angew Chemistry, Int Edit, 55(2016)14668-14672.
- [21] P. Simon, Y. Gogotsi, B. Dunn, Where Do Batteries End and Supercapacitors Begin?, Science, 343 (2014) 1210-1211.
- [22] Y. Chang, Y. W. Sui, J. Q. Qi, L. Y. Jiang, Y. Z. He, F. X. Wei, Q. K. Meng, Y. X. Jin, Facile synthesis of  $\text{Ni}_3\text{S}_2$  and  $\text{Co}_9\text{S}_8$  double-size nanoparticles decorated on rGO for high-performance supercapacitor electrode materials, Electrochemical Acta, 226 (2017)69-78.
- [23] G. Wang, L. Zhang, J. Zhang, A review of electrode materials for electrochemical supercapacitors. Chem. Soc. Review. 41 (2012) 797-828.
- [24] K. Jost, C. R. Perez, J. K. McDonough, V. Presser, M. Heon, G. Dion, Y. Gogotsi, Carbon coated textiles for flexible energy storage, Energy Environmental Science, 4 (2011) 5060-5067.
- [25] H. Wu, Y. Zhang, L. Cheng, L. Zheng, Y. Li, W. Yuan, X. Yuan, Graphene based architectures for electrochemical capacitors, Energy Storage Materials, 5 (2016) 8-32.
- [26] X.-Y. Liu, K.-X. Wang, J.-S. Chen, Template-directed metal oxides for electrochemical energy storage, Energy Storage Mater. 3 (2016) 1-17.
- [27] Y. Murakami, T. Kondo, Y. Shimoda, H. Kaji, K. Yahikozawa, Y. Takasu, Effects of rare earth chlorides on the preparation of porous ruthenium oxide electrodes, J. Alloys. Comp. 239(1996)111-113.
- [28] C.-C. Hu, W.-C. Chen, Effects of substrates on the capacitive performance of  $\text{RuO}_x \cdot n\text{H}_2\text{O}$  and activated carbon- $\text{RuO}_x$  electrodes for supercapacitors, Electrochemical Acta 49 (2004) 3469-3477.
- [29] Y.-J. Yang, E.-H. Liu, L.-M. Li, Z.-Z. Huang, H.-J. Shen, X.-X. Xiang, High Rate Performance Nanocomposite Electrode of Mesoporous Manganese Dioxide/Silver Nanowires in KI Electrolytes, Journal of Alloys and Comp. 505 (2010) 555-559.
- [30] X. Wang, Y. Li, Selected-Control Hydrothermal Synthesis of  $\alpha$ - and  $\beta$ - $\text{MnO}_2$  Single Crystal Nanowires, Journal of Am. Chem. Soc. 124 (2002) 2880-2881.



- [31] M. Wu, J. Gao, S. Zhang, A. Chen, Special issue including selected papers from the 3rd International Conference on Materials for Advanced Technologies (ICMAT 2005, Singapore, Malaysia) and the Summer School on Synthesis of Nanostructured Materials for Polymer Batteries (Augustów, Poland) together with regular papers, *Journal of Power Sources* 159 (2006)365-369.
- [32] X. Yan, X. Tong, J. Wang, C. Gong, M. Zhang, L. Liang, *Electrochemical Capacitors: Theory, Materials and Applications*, *Journal of Alloys Compound* 593 (2014)184-189.
- [33] S. K. Meher, G. R. Rao, Ultra layered  $\text{Co}_3\text{O}_4$  for High-Performance Supercapacitor Applications, *Journal of Physical Chemistry*,115(2011)15646-15654.
- [34] V. Srinivasan, J. W. Weidner, Capacitance studies of cobalt oxide films formed via electrochemical precipitation, *Journal of Power Sources* 108 (2002) 15-20.
- [35] Y. Zhu, X. Ji, C. Pan, Q. Sun, W. Song, L. Fang, Q. Chen, C. E. Banks, A carbon quantum dot decorated  $\text{RuO}_2$  network: outstanding supercapacitances under ultrafast charge and discharge, *Energy Environmental Science*, 6 (2013) 3665-3675.
- [36] Xiu Feng Han, Shahzadi Shamaila and Rehana Sharif, *Ferromagnetic Nanowires and Nanotubes*, Institute of Physics, Chinese Academy of Sciences, Beijing 100190 China.
- [37] Kalyani M, Emerson R.N.\*, *Electrodeposition of nano crystalline cobalt oxide on porous copper electrode for supercapacitor*, *Journal of Materials Science: Materials in Electronics*, (2018) Springer Science+Business Media, LLC, part of Springer Nature, [doi.org/10.1007/s10854-018-0389-y](https://doi.org/10.1007/s10854-018-0389-y).
- [38] R. Venkatesha, C. Ravi Dhasa\*, R. Sivakumarb, T. Dhandayuthapanib, P. Sudhagarc, C. Sanjeevirajad, A. Moses Ezhil Raj, Analysis of optical dispersion parameters and electrochromic properties of manganese-doped  $\text{Co}_3\text{O}_4$  dendrite structured thin films. *Journals of physics and chemistry of solids* 122 (2018) 118-129.
- [39] J. Hu, M. Li, F. Lv, M. Yang, P. Tao, Y. Tang, H. Liu, Z. Lu, Heterogeneous  $\text{NiCo}_2\text{O}_4$ @polypyrrole core/sheath nanowire arrays on Ni foam for high performance supercapacitors, *Journal of Power Sources* 294 (2015) 120.
- [40] F. Han, D. Li, W.-C. Li, C. Lei, Q. Sun, A.-H. Lu, Nano engineered poly pyrrole coated  $\text{Fe}_2\text{O}_3$ @C multifunctional composites with an improved cycle stability as lithium-ion anodes, *Adv. Funct. Mater.* 23 (2013) 1692.
- [41] C. Xu, J. Sun, L. Gao, Synthesis of novel hierarchical graphene/poly pyrrole nano sheet composites and their superior electrochemical performance, *J. Mater. Chem.* 21 (2011) 11253.
- [42] Shaymaa Al-Rubaye, Ranjusha Rajagopalan\*, Chandrasekar M. Subramaniam, Zheyin Yu, Shi Xue Dou, Zhenxiang Cheng, Electrochemical performance enhancement in  $\text{MnCo}_2\text{O}_4$  nano flake/graphene nano platelets composite, *Journal of Power Sources* 324 (2016) 179-187.
- [43] K.K. Purushothaman, B. Sethuraman, M.P. Anupama, M. Dhanasankar, G. Muralidharan, Optical, structural, and electrochromic properties of cobalt oxide films prepared via the sol-gel route, *Material Science Semiconductors Process.* 16 (2013) 1410-1415.
- [44] X.H. Xia, J.P. Tu, J. Zhang, X.H. Huang, X.L. Wang, W.K. Zhang, H. Huang, Enhanced electrochromics of nanoporous cobalt oxide thin film prepared by a facile chemical bath deposition, *Electrochemistry Communication*,10 (2008) 1815-1818.
- [45] Naveen AN, Selladurai S (2014), Investigation on physiochemical properties of Mn substituted spinel cobalt oxide for supercapacitor applications. *Electrochemical Acta*, 125:404-414.
- [46] R.C. Ambare a, S.R. Bharadwaj b, B.J. Lokhande, Electrochemical characterization of  $\text{Mn}:\text{Co}_3\text{O}_4$  thin films prepared by spray pyrolysis via aqueous route, *Current Applied Physics* 14 (2014) 1582-1590.



10.22214/IJRASET



45.98



IMPACT FACTOR:  
7.129



IMPACT FACTOR:  
7.429



# INTERNATIONAL JOURNAL FOR RESEARCH

IN APPLIED SCIENCE & ENGINEERING TECHNOLOGY

Call : 08813907089  (24\*7 Support on Whatsapp)